# Antifog coating for bronchoscope lens

**R. L. Leonard[1], A. Y. Terekhov[1], C. Thompson[2], R. A. Erck[3] and J. A. Johnson*[1]**

Current bronchoscopes suffer from fogging and the adhesion of mucus plugs to the lens. A doped diamond-like carbon film was developed as a possible solution to this problem. A silicon monoxide dopant was found to produce a film that was transparent, hydrophilic and stable in simulated body fluid (SBF) and therefore showed potential as an antifogging coating. The film was deposited by pulsed laser deposition and characterised by Raman spectroscopy, atomic force microscopy, spectrophotometry and contact angle measurements. Root mean square surface roughness was found to be <1 nm. The unique characteristics of these films include production without secondary processing, a lowest contact angle of 25° and stability in SBF for several months combined with transparency.

**Keywords:** Coating, Doping, Characterisation, Biomedical, Carbon

## Introduction

When optical windows move from a cold to a warm environment, water tends to condense on the surface, causing the window to fog over, greatly reducing visibility. This is problematic for medical instruments, such as the bronchoscope, which suffer from fogging and the adhesion of mucus plugs to the lens. Current antifogging lenses use a surfactant to reduce the surface tension of the liquid on the lens. The water spreads out evenly instead of beading up, letting light pass through without scattering, which allows the lens to be transparent. The major drawback to this approach is that the effects are not permanent and the surfactant must be reapplied periodically. An improvement would be to apply a permanent hydrophilic coating to the surface of the lens.

The contact angle of water on a solid surface is related to the surface energy of the material. High surface energy materials such as metals and ceramics are hydrophilic and achieve a much higher degree of wetting than low surface energy materials such as polymers. Surface energy is given by the following equation

$$\gamma = \gamma^{d} + \gamma^{p} + \gamma^{h} \quad (1)$$

where $\gamma$ is the surface energy, $d$ is the dispersive force, $p$ is the polar force and $h$ is the hydrogen bonding.[1,2]

Diamond-like carbon (DLC) films are versatile and biocompatible[3,4] and can be doped to modify their properties.[5–9] Some dopants, such as nitrogen, oxygen and fluorine, can increase surface energy due to their capability to form hydrogen bonds.[6,10,11] Potential dopants in this work had to meet criteria pertaining to insertion into the human body, as well as being capable of incorporation into a pulsed laser deposition (PLD) ablation target.

Titanium dioxide and silicon monoxide doped DLCs on fused silica substrates were evaluated as potential biocompatible antifog coatings. The films were characterised by Raman spectroscopy, atomic force microscopy (AFM), spectrophotometry and contact angle measurements. The stability of the films was tested in simulated body fluid (SBF).

## Experimental

The films were deposited on fused silica (University Wafer, UV grade) 25·4 mm square substrates of 500 μm thickness. The substrates were ultrasonically cleaned in acetone (Alfa Aesar, assay 99·5%) and methanol (Fisher Chemical, assay ⩾99·8%) in separate steps followed by a 2 min dip in piranha solution that consisted of a 1 : 1 volume ratio of $H_2SO_4$ (Acros Organics, 95% solution in $H_2O$) and $H_2O_2$ (Kor-Chem, Inc., 35 wt-% in $H_2O$). Rinsing with ultrapure water and drying with compressed argon were performed after each step.

The DLC films were deposited with the PLD system (shown in Fig. 1) using a 193 nm ArF excimer laser having a repetition rate of 50 Hz and a pulse length of 15 ns. The laser pulse energy was 4·0 mJ, creating a fluence of $3{\cdot}1 \pm 0{\cdot}2$ J cm$^{-2}$ when focused on an area of the target measuring 0·13 mm$^2$; the target was rotated and translated during deposition. The vacuum chamber pressure was $1{\cdot}0 \times 10^{-6}$ torr or lower.

For dopant incorporation into the DLC, multicomponent targets comprised of graphite (Poco Graphite, Inc., semiconductor grade, TRA-1) and the desired doping material, SiO (Kurt J. Lesker Co., 99·9% pure) or $TiO_2$ (Kurt J. Lesker Co., 99·9% pure), were used. A 50·8 mm diameter graphite target with a 90° cut-out was paired with a wedge shaped piece of the desired doping material and a wedge shaped graphite spacer (*see* Fig. 2). For the undoped film, a solid 360° graphite target was used. Deposition time was 4 h for the doped samples and 15 min for the undoped sample, as longer times caused delamination due to residual

[1]The University of Tennessee Space Institute, Tullahoma, TN 37388, USA
[2]Northern Illinois University, DeKalb, IL 60115, USA
[3]Argonne National Laboratory, Argonne, IL 60439, USA

*Corresponding author, email jjohnson@utsi.edu

© 2012 Institute of Materials, Minerals and Mining
Published by Maney on behalf of the Institute
Received 25 December 2011; accepted 27 February 2012
DOI 10.1179/1743294412Y.0000000007

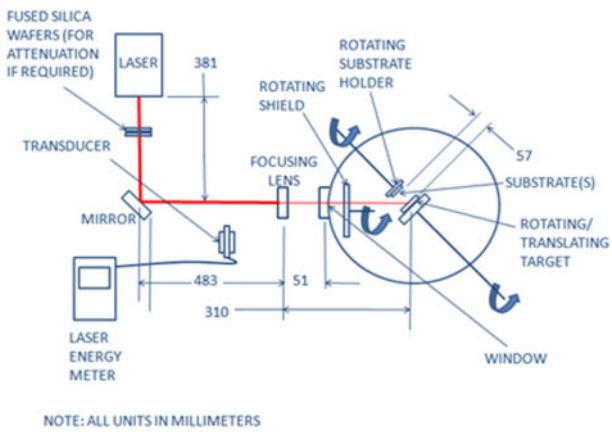


**1 Schematic of deposition system**

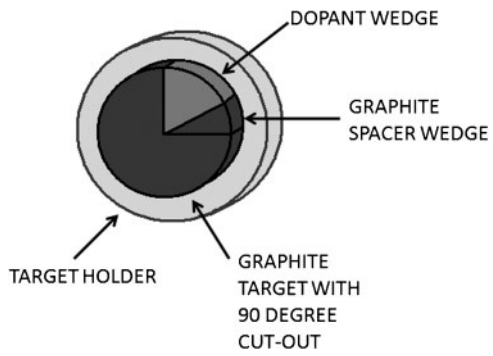


**2 Schematic of target holder with dopant wedge installed**

stresses. The substrate temperature for all depositions was $19 \pm 2^{\circ}$C.

Film thickness was measured using an optical profilometer, which was a Phase Shift Technology Micro-XAM surface mapping microscope (Tucson, AZ) connected to a personal computer with MapVue AE 1·24·1 software. Measurements were made at a minimum of two locations per sample.

Raman spectroscopy was performed on all samples using a Renishaw inVia Raman microscope (New Mills, Wotton-under-Edge, Gloucestershire, UK). The laser was focused through a $\times 50$ lens and had a power of 4 mW. The laser wavelength was 633 nm. Acquisition was for 10 s, with ten accumulations at each location measured.

Simulated body fluid, which has ion concentrations similar to that found in human blood plasma, was prepared as described by Cho *et al.*[12] Samples were immersed in vials containing SBF and incubated at 36·5°C using a temperature controlled water bath. After varying intervals of time, the samples were removed and photographed microscopically. The samples were then placed in fresh SBF and returned to the 36·5°C environment.

Topography of the samples was measured using a VEECO Nanoscope V atomic force microscope (Plainview, NY). The system was equipped with a nitrogen gas vibration isolation stage and an acoustic/Faraday cover. The AFM was also equipped with a Nanoscope V controller and a computer with Nanoscope 7·30 software. All images were taken under ambient conditions using silicon tips in tapping mode. Analysis was performed using WSxM 4·0 Beta 2·0 software.[13]

The contact angle of water was measured using a Krüss DSA20E Easy Drop Standard with a software controlled dosing system (Hamburg, Germany). Measurements were made at five locations per sample using the sessile drop method with a drop size of 2 μL. The average contact angle for each film was determined along with the standard error.

Spectrophotometry data were obtained by using a GenTech Scientific TU-1901 double beam ultraviolet/visible light spectrophotometer equipped with UVWin5·0 analysis software (Arcade, NY). The transparency of DLC on fused silica substrates was measured between 190 and 900 nm at 1·0 nm intervals. The attenuation effects of the substrate were subtracted from the transmittance plots using a bare fused silica substrate as reference during the measurements.

## Results and discussion

The thickness and growth rate results for the DLC films produced are shown in Table 1. The addition of the dopant material led to a reduction of residual stresses typically found in DLC films and allowed for thicker films to be produced without delamination. The doped films have a much lower growth rate than the undoped film; the addition of dopant material appears to drastically impede the growth rate of the films. However, there is no clear relationship between the dopant level and the film growth rate.

Dopants not only change the composition of the films but may also alter the nature of the carbon bonding within. The Raman spectrum for DLC films can be deconvoluted into two Gaussian peaks known as D peak and G peak, which are located at approximately 1350 and 1580 $cm^{-1}$ respectively, when excited by visible

**Table 1 Film thickness and deposition rate for doped and undoped DLC films**

| Sample PLD # | Dopant | Wedge size/° | Deposition time/min | Thickness/nm | Deposition rate/nm $min^{-1}$ |
|---|---|---|---|---|---|
| 57 | $TiO_2$ | 30 | 240 | $165 \pm 13$ | $0{\cdot}69 \pm 0{\cdot}06$ |
| 59 | $TiO_2$ | 35 | 240 | $146 \pm 10$ | $0{\cdot}61 \pm 0{\cdot}04$ |
| 56 | $TiO_2$ | 40 | 240 | $169 \pm 13$ | $0{\cdot}70 \pm 0{\cdot}06$ |
| 60 | $TiO_2$ | 45 | 240 | $194 \pm 7$ | $0{\cdot}81 \pm 0{\cdot}03$ |
| 55 | $TiO_2$ | 50 | 240 | $187 \pm 5$ | $0{\cdot}78 \pm 0{\cdot}03$ |
| 58 | $TiO_2$ | 55 | 240 | $146 \pm 14$ | $0{\cdot}61 \pm 0{\cdot}06$ |
| 63 | SiO | 30 | 240 | $191 \pm 13$ | $0{\cdot}80 \pm 0{\cdot}05$ |
| 59 | SiO | 35 | 240 | $158 \pm 11$ | $0{\cdot}66 \pm 0{\cdot}05$ |
| 62 | SiO | 40 | 240 | $179 \pm 4$ | $0{\cdot}75 \pm 0{\cdot}02$ |
| 60 | SiO | 45 | 240 | $217 \pm 7$ | $0{\cdot}90 \pm 0{\cdot}03$ |
| 66 | SiO | 50 | 240 | $114 \pm 9$ | $0{\cdot}47 \pm 0{\cdot}04$ |
| 64 | SiO | 55 | 240 | $119 \pm 10$ | $0{\cdot}50 \pm 0{\cdot}04$ |
| 42 | None | n/a | 15 | $27 \pm 1$ | $1{\cdot}8 \pm 0{\cdot}1$ |

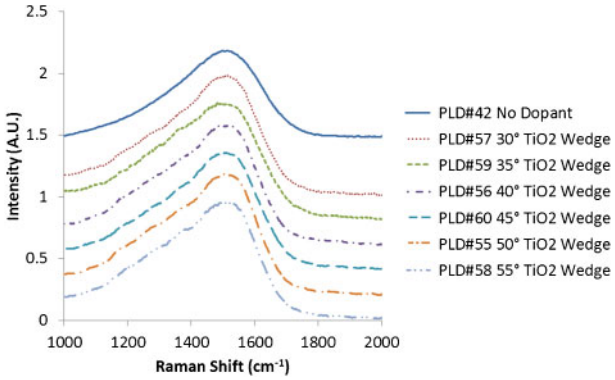


**3 Raman spectra of DLC films produced with varying amounts of titanium dioxide dopant**

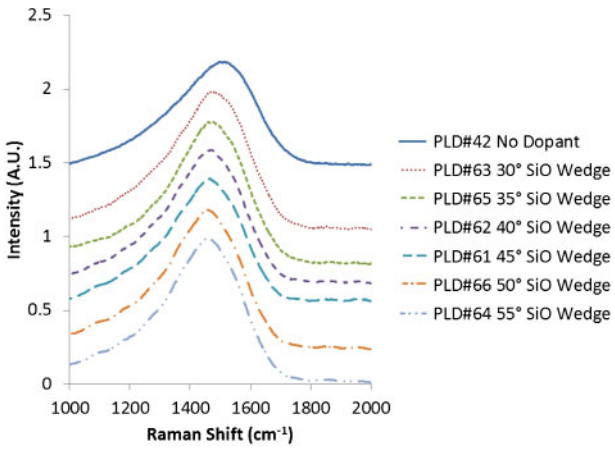


**4 Raman spectra of DLC films produced with varying amounts of silicon monoxide dopant**

light.[14] The relative intensity of these peaks ($I_D/I_G$) and the full width half maximum and position of the G peak are thought to give insight to the $sp^3/sp^2$ ratio of hybrid bonding in DLC films. It has been demonstrated that increased full width half maximum of the G peak and decreased G peak position and $I_D/I_G$ ratios are indicative of an increased $sp^3/sp^2$ bonding ratio within undoped DLC films.

The Raman spectra for titanium dioxide doped DLC films are shown in Fig. 3. Deconvolution of the spectra yields the peak characteristics shown in Table 2. There appears to be little change in peak characteristics with increasing amounts of dopant. The films all have lower G peak positions, larger ratios of intensity between the

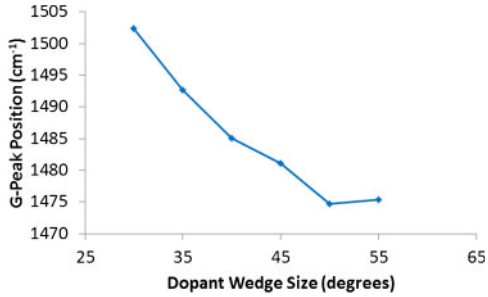


**5 Relationship between silicon monoxide dopant wedge and G peak position in Raman spectra of silicon monoxide doped films**

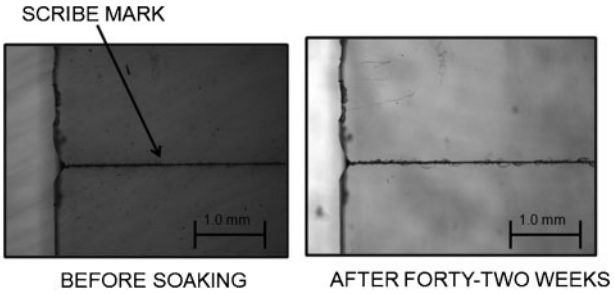


**6 Optical micrograph of silicon monoxide doped DLC film, PLD #61, before soaking and after 42 weeks of immersion in SBF**

D and G peaks and narrower G peak widths than the undoped DLC film (PLD #42) made under similar conditions. These differences, though, are slight.

For silicon monoxide doped DLC, the Raman spectra for the films are shown in Fig. 4. The peak characteristics are also shown in Table 2. The only relationship revealed is that between dopant content and G peak position, as shown in Fig. 5. The decreasing G peak position may be indicative of an increased $sp^3/sp^2$ bonding ratio and increased diamond-like character.

For use on bronchoscope lenses, the films should remain biocompatible after doping and be stable within the human body. *In vitro* testing in SBF provides a straightforward way to determine the stability of the films. Sample PLD #61, a silicon monoxide doped DLC film, is shown in Fig. 6 after 42 weeks of soaking in SBF. No significant change was observed in the film, even at an interface between the DLC and fused silica exposed by a scribe mark that was made before soaking began. Any anomalies seen were attributed to handling

**Table 2 Raman spectra characteristics for doped and undoped DLC films**

| Sample PLD # | Dopant | Wedge/° | G peak position | $I_D/I_G$ | Full width half maximum G peak |
|---|---|---|---|---|---|
| 57 | $TiO_2$ | 30 | 1527·9±0·3 | 0·85±0·01 | 201·8±1·5 |
| 59 | $TiO_2$ | 35 | 1529·2±0·6 | 1·04±0·04 | 213·5±4·0 |
| 56 | $TiO_2$ | 40 | 1529·2±0·3 | 0·97±0·01 | 187·0±1·3 |
| 60 | $TiO_2$ | 45 | 1527·7±0·3 | 0·88±0·01 | 201·1±1·4 |
| 55 | $TiO_2$ | 50 | 1530·6±0·3 | 0·96±0·01 | 184·0±1·2 |
| 58 | $TiO_2$ | 55 | 1530·1±0·3 | 1·02±0·03 | 209·4±2·8 |
| 63 | SiO | 30 | 1502·4±1·9 | 0·48±0·02 | 220·0±4·1 |
| 59 | SiO | 35 | 1492·7±4·6 | 0·43±0·03 | 206·3±8·2 |
| 62 | SiO | 40 | 1485·1±1·4 | 0·44±0·01 | 229·5±3·8 |
| 60 | SiO | 45 | 1481·1±0·9 | 0·77±0·02 | 209·4±2·8 |
| 66 | SiO | 50 | 1474·7±1·9 | 0·40±0·01 | 224·2±4·0 |
| 64 | SiO | 55 | 1475·4±2·4 | 0·40±0·02 | 219·1±5·0 |
| 42 | None | n/a | 1537·0±0·9 | 0·77±0·04 | 218·4±5·5 |

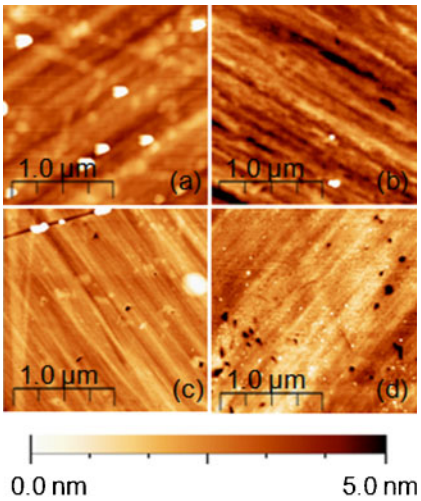


**7 Images (AFM) of *a* PLD #60, DLC doped with titanium dioxide, *b* PLD #63, DLC doped with silicon monoxide, *c* PLD #42, undoped DLC and *d* bare fused silica substrate**

damage. Films of DLC with titanium dioxide were not stable and delaminated over time while soaking.

Roughness can affect the contact angle, so it must be considered when evaluating a film to be used as an antifogging coating.[15] Therefore, AFM measurements were made for the doped DLC films (*see* Fig. 7). Striations can be seen across the films' surfaces, similar to those found on bare fused silica substrates. This similarity indicates that the roughness of the underlying substrate influences the roughness of the surface of the films. Although not ideal, some general information can still be obtained regarding the surface characteristics of the films. The surface roughness values for the doped films are shown in Fig. 8. They have surface roughness values similar to that of undoped film PLD #42, which has a root mean square roughness of 0·52 nm. Any changes in the contact angle found with the addition of dopants are likely to be due to only changes in the surface energy because of the similarity in the surface roughness values for both doped and undoped films.

Small particulates can be seen in the AFM images of the titanium dioxide doped films. These particulates may have been created as a result of the ablation process and

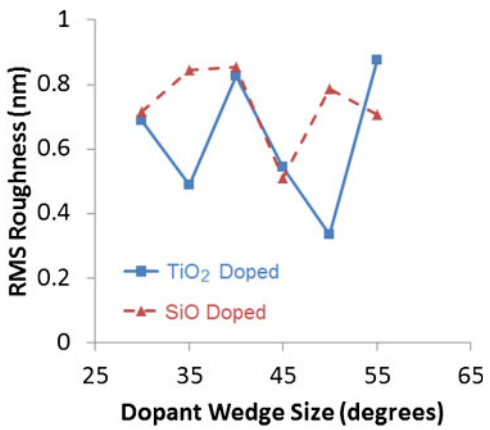


**8 Root mean square roughness for DLC films doped with titanium dioxide and silicon monoxide as function of dopant wedge size**

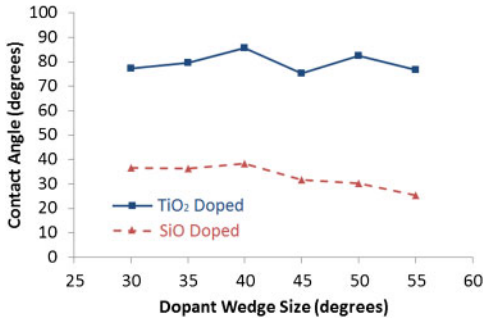


**9 Contact angle as function of dopant wedge size for titanium dioxide and silicon monoxide doped DLC films**

give indication that the films are not homogeneous in the submicrometre scale.

The AFM results for the silicon monoxide doped films show surfaces that are generally free of particulates on a nanometre scale. This indicates that the DLC matrix was formed on the subatomic, atomic or molecular scale from electrons, atoms, ions and/or molecules contained within the ablation plume, created from the carbon and silicon monoxide composite target. Because the rotating target had two chemically distinct regions, the composition of the ablation plume periodically alternated between the carbon, silicon and oxygen species, which bonded covalently to the fused silica substrate and subsequent growth layers. Because the films possess striations similar to the uncoated substrate, the films are thought to have formed through layer by layer growth.

The results, pertaining to the contact angle, of doping DLC with titanium dioxide can be seen in Fig. 9. They are similar to that of the undoped film PLD #42, which has a contact angle of 76·9°. Furthermore, there is no pattern of increasing or decreasing contact angle with increased dopant. It is therefore concluded that the addition of titanium dioxide has no effect on the contact angle for DLC films, and the dopant is not useful for the proposed purpose.

The addition of silicon monoxide dopant into DLC films had a marked effect on the contact angle, as shown in Fig. 9. Diamond-like carbon film sample PLD #64, with a 55° silicon monoxide dopant wedge, achieved a very small hydrophilic contact angle of 25°, much lower than previously quoted values.[16] It should be noted that the contact angle decreases with increasing silicon monoxide dopant content. This trend suggests that further increasing the silicon monoxide doping could produce even lower contact angles.

The contact angle measurements for the samples were performed >2 weeks after their synthesis. During this time, the samples were exposed intermittently to ambient air, indicating that the hydrophilic nature of the samples is not short lived. Future studies will include periodic retesting of the samples to determine the permanency of their hydrophilic nature.

Measuring the contact angle of other probe liquids, in addition to water, on both doped and undoped film surfaces would be beneficial. These measurements using multiple probe liquids would allow the surface energy of the film to be calculated.[17]

The DLC films doped with silicon monoxide, a blackish brown amorphous material, block the transmission of far ultraviolet light, as shown in Fig. 10, but transmit quite well in the far infrared.

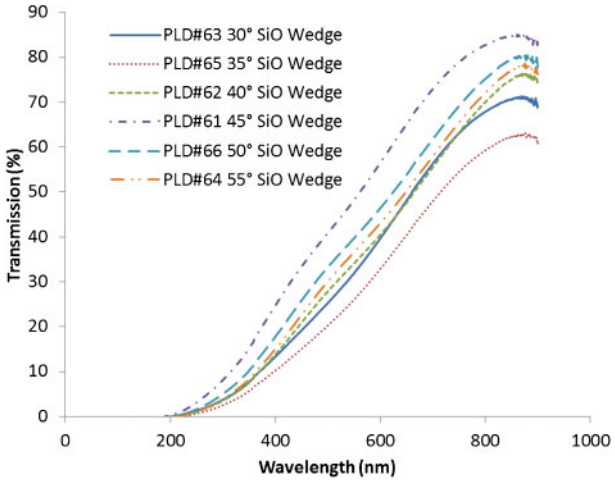


**10 Transmittance of DLC films made with varying amounts of silicon monoxide dopant**

## Conclusion

The DLC films produced with titanium dioxide dopant did not demonstrate a significant decrease in contact angle and do not warrant further research for antifogging applications.

Doping DLC films with silicon monoxide led to a marked decrease in contact angle of water on the films, producing angles as low as 25°. The data suggest that further reduction in contact angle may be possible with increased silicon monoxide dopant. The results indicate that DLC films doped with silicon monoxide show potential for use in antifogging applications, such as bronchoscope lenses, due to their transparency, stability and low contact angle.

## Acknowledgements

The authors would like to acknowledge the Center for Nanoscale Materials at Argonne National Laboratory for use of its Raman microscope. Use of the Center for Nanoscale Materials was supported by the US Department of Energy, Office of Science, Office of Basic Energy Sciences, under contract no. DE-AC02-06CH11357.

## References

1. S. Zhang and N. Ali: 'Nanocomposite thin films and coatings'; 2007, Danvers, MA, Imperial College Press.
2. Y. Nitta, K. Okamoto, T. Nakatani and A. Mochizuki: 'Development of novel DLC film using plasma technique for medical material', *J. Photopolym. Sci. Technol.*, 2010, **23**, (2), 245–250.
3. S. Sahoo, S. S. Pradhan, V. Bhavanasi and S. K. Pradhan: 'Structural and mechanical characterization of diamond like carbon films grown by microwave plasma CVD', *Surf. Coat. Technol.*, 2010, **204**, (16–17), 2817–2821.
4. E. Pecheva, L. Pramatarova, D. Fingarova, T. Hikov, I. Dineva, Z. Karagyozova and S. Stavrev: 'Advanced materials for metal implant coatings', *J. Optoelectron. Adv. Mater.*, 2009, **11**, (9), 1323–1326.
5. M. Grischke, K. Bewilogua, K. Trojan and H. Dimigen: 'Application-oriented modifications of deposition processes for diamond-like-carbon-based coatings', *Surf. Coat. Technol.*, 1995, **74–75**, 739–745.
6. S. F. Ahmed, D. Banerjee and K. K. Chattopadhyay: 'The influence of fluorine doping on the optical properties of diamond-like carbon thin films', *Vacuum*, 2010, **84**, (6), 837–842.
7. S. F. Ahmed, M. W. Moon and K. R. Lee: 'Effect of silver doping on optical property of diamond like carbon films', *Thin Solid Films*, 2009, **517**, (14), 4035–4038.
8. S. M. Baek, T. Shirafuji, N. Saito and O. Takai: 'Adhesion property of SiO(x)-doped diamond-like carbon films deposited on polycarbonate by inductively coupled plasma chemical vapor deposition', *Thin Solid Films*, 2011, **519**, (20), 6678–6682.
9. S. M. Baek, T. Shirafuji, N. Saito and O. Takai: 'Fabrication of transparent protective diamond-like carbon films on polymer', *Jpn. J. Appl. Phys.*, 2011, **50**, (8), 08JD08–08JD08-5.
10. H. Akasaka, T. Yamada and N. Ohtake: 'Effect of film structure on field emission properties of nitrogen doped hydrogenated amorphous carbon films', *Diamond Relat. Mater.*, 2009, **18**, (2–3), 423–425.
11. Y. T. Kim, S. G. Yoon, S. J. Suh, J. H. Lee, G. E. Jang and D. H. Yoon: 'The effect of $H_2$, $N_2$ and $N_2O$ doping on DLC thin films deposited by a PECVD method', *J. Ceram. Process. Res.*, 2005, **6**, (3), 205–208.
12. S. Cho, K. Nakanishi, T. Kokubo and N. Soga: 'Dependence of apatite formation on silica gel on its structure: effect of heat treatment', *J. Am. Ceram. Soc.*, 1995, **78**, (7), 1769–1774.
13. I. Horcas, R. Fernadez, J. Gomez-Rodrigues, J. Colchero, J. Gomez-Herrero and A. Baro: 'WSXM: a software for scanning probe microscopy and a tool for nanotechnology', *Rev. Sci. Instrum.*, 2007, **78**, (013705), 1–8.
14. W. G. Cui, Q. B. Lai, L. Zhang and F. M. Wang: 'Quantitative measurements of sp(3) content in DLC films with Raman spectroscopy', *Surf. Coat. Technol.*, 2010, **205**, (7), 1995–1999.
15. S. Nagashima, T. Hasebe, A. Kamijo, Y. Yoshimoto, A. Hotta, H. Morita, H. Terada, M. Tanaka, K. Takahashi and T. Suzuki: 'Effect of oxygen plasma treatment on non-thrombogenicity of diamond-like carbon films', *Diamond Relat. Mater.*, 2010, **19**, (7–9), 861–865.
16. S. Meskinis, R. Gudaitis, K. Slapikas, S. Tamulevicius, M. Andrulevicius, A. Guobiene, J. Puiso and G. Niaura: 'Ion beam energy effects on structure and properties of SiO(x) doped diamond-like carbon films', *Surf. Coat. Technol.*, 2008, **202**, (11), 2328–2331.
17. M. Zenkiewicz: 'Methods for the calculation of surface free energy of solids', *JAMME*, 2007, **24**, (1), 137–145.